Deep Learning approach to Human Osteosarcoma Cell Detection and Classification

Mario D'Acunto[1], Massimo Martinelli[2], and Davide Moroni[2]

[1] Institute of Biophysics
National Research Council of Italy, Via Moruzzi, 1 – 56124-Pisa (IT)
mario.dacunto@pi.ibf.cnr.it
[2] Institute of Information Science and Technologies,
National Research Council of Italy, Via Moruzzi, 1 – 56124-Pisa (IT)
Name.Surname@isti.cnr.it

Abstract. The early diagnosis of a cancer type is a fundamental goal in cancer treatment, as it can facilitate the subsequent clinical management of patients. The leading importance of classifying cancer patients into high or low risk groups has led many research teams, both from biomedical and bioinformatics field, to study the application of Deep Learning (DL) methods. The ability of DL tools to detect key features from complex datasets is a fundamental achievement in early diagnosis and cell cancer progression. In this paper, we apply DL approach to classification of osteosarcoma cells. Osteosarcoma is the most common bone cancer occurring prevalently in children or young adults. Glass slides of different cell populations were cultured from Mesenchimal Stromal Cells (MSCs) and differentiated in healthy bone cells (osteoblasts) or osteosarcoma cells. Images of such samples are recorded with an optical microscope. DL is then applied to identify and classify single cells. The results show a classification accuracy of 0.97. The next step is the application of our DL approach to tissue in order to improve digital histopathology.

Keywords: Osteosarcoma Cells, Deep Learning, Convolutional Neural Networks, Convolutional Object Detection Systems, Cell Classification

1 Introduction

Over the last decades, scientists applied different methods to detect cancer tissues at the early stage. This is because early diagnosis can facilitate the clinical managements of patients. Early diagnosis requires the ability to identify cancer tissue as small as a single cell. Classification of cancer cells is hence key research for early diagnosis and for identification of differentiation and progression of cancer in a single cell [14] [7] [11] . With advent of new digital technologies in the field of medicine, Artificial Intelligence (AI) methods have been applied in cancer research to complex datasets in order to discover and identify patterns and relationships between them. Machine Learning (ML) is a branch of AI related to the problem of learning from data samples to the general concept of inference. The main objective of ML techniques is to produce a model, which can be

used to perform classification, prediction, estimation or any other similar task. When a classification model is developed, by means of ML techniques, training and generalization errors can be dealt out. The former refers to misclassification errors on the training data while the latter on the expected errors on testing data. A good classification model should fit the training set well and accurately classify all the instances. Once a classification model is obtained using one or more ML techniques, it is necessary to estimate the classifier's performance. The performance analysis of each proposed model is measured in terms of sensitivity, specificity, accuracy, and so-called area under the curve (AUC). Sensitivity is usually defined as the proportion of true positives that are correctly observed by the classifier, whereas specificity is defined as the proportion of true negatives that are correctly identified. In turn, accuracy, that is a measure related to the number of correct predictions, and AUC, that is a measure of model's performance, are used for assessing the overall performance of a classifier. DL is a part of ML methods based on learning data representation. Inside DL, Convolutional Object Detection (COD) is a recent approach to cancer analysis. In this paper, we have applied a COD-based DL method to several differentiated samples of cells cultured on glass slide, with the purpose to discriminate osteosarcoma cells from MSCs (osteoblasts). The results show excellent performance with an accuracy of nearly 1. The next step will be to extend the algorithm to large populations of cells and tissues with the purpose to improve digital histopathology. In section 2 a related works are described. Section 3 describes cell culture, how was built e handled the dataset and the network used for detection and classification. Section 4 shows the results of training and accuracy of the method applied. Section 5 summarizes our conclusions.

2 Related works

Image-based ML and, in particular, DL have recently shown expert-level accuracy in medical image classification, ranging from ophtalmology to diagnostic pathology [2]. Within digital pathology, quantification and classification of digitized tissue samples by supervised deep learning has shown good results even for tasks previously considered too challenging to be accomplished with conventional image analysis methods [3, 18, 8–10, 5].

Many tasks in digital pathology, such as counting mitoses, quantifying tumor infiltrating immune cells, or tumor cell differentiation require the classification of small clusters of cells up to single cell, if possible. For this purpose, we have addressed our efforts to classify cultured cells with known grade of differentiation with a supervised DL.

COD is a very recent technique of machine learning for the analysis of cancer. A number of methods have been proposed to address the object recognition task and many software frameworks have been implemented to develop and work with deep learning networks (such as Caffe, Apache MXNet and many others).

Among all such methods, Google TensorFlow is currently on e of the most used framework and its Object Detection API emerged as a very powerful tool for image recognition.

In [6] a guide for selecting the right architecture depending on speed, memory and accuracy is provided.

Since our case requires the highest accuracy architecture allowable, we selected the Faster Region Convolutional Neural Network (Faster R-CNN) [12, 13] that is a recent region proposal network sharing features with the detection network that improves both region proposal quality and object detection accuracy.

Faster R-CNN uses two networks: a Region Proposal Network (RPN) to generate region proposals and a detector network to discover object. The RPN generates region proposals more quickly than the Selective Search [17] algorithm used in previous solutions. By sharing information between the two networks, the accuracy is also improved and this solution is currently the one with the best results in the latest object detection competitions.

3 Material and Methods

3.1 Cells Culture

Normal, cancerous and mixed cells were cultured on glass slides, as follows:

i) Undifferentiated MSCs were isolated from human bone marrow according to a previously reported method [15] and used to perform three culture strategies. MSCs were plated on glass slides inside Petri dishes at a density of 20,000 cells with 10% fetal bovine serum (FBS). The samples were cultured for 72 h, then fixed in 1% neutral buffered formalin for 10 min at 4°C.

ii) Osteosarcoma cells. MG-63 (human osteosarcoma cell line ATCC CRL-1427) cells were seeded on 6 glass slides at 10,000 cells in Eagle's Minimum Essential Medium (EMEM) supplemented with 10% FBS and cultured for 72h; thereafter the samples were formalin fixed, as in i).

iii) Mixed cancer and normal cells. MSCs were plated on 6 glass slides inside Petri dishes at 10,000 cells with 10% FBS. In parallel, MG-63 cells were plated at passage 2 on 6 well tissue culture plate (50,000 cells/2 ml) in EMEM supplemented with 10% FBS. After 24 h, the MG-63 cells were harvested and seeded at 10,000 cells onto glass slides previously seeded with MSCs. After 72h the glass slides were formalin fixed, as in i).

At each endpoint, all the samples were fixed in 1% (w/v) neutral buffered formalin for 10min at 4°C.

Morphologies are visible in Figure 1, as imaged by an inverted microscope (Nikon Eclipse Ti-E).

3.2 Data set collection and annotation

Collected images have been divided into two groups, a test set and a validation set. The test set images have been labeled by the domain expert using the LabelImg Software [16].

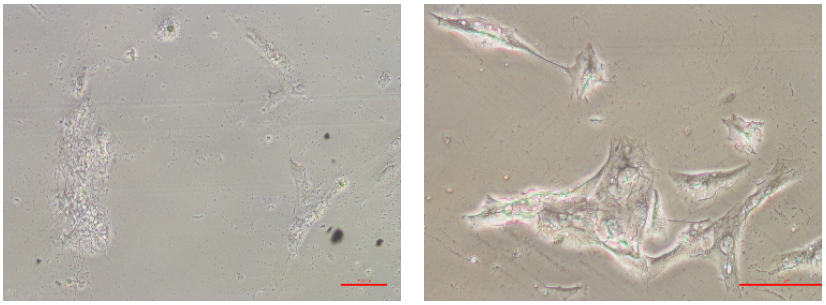

Fig. 1. Morphology of osteoblast cells, (left, 10× objective, scale bar 100μm), and osteosarcoma cells (right, 20× objective, scale bar 50μm).

Overall 229 objects where labeled in 48 images used for training, and 12 were used for validation, that is the size ratio of the classification network in comparison to the size of the training was 80/20.
Categories used to label were five:

- single cancer cell
- cancer_cluster
- single MSC cell
- MSC_cluster
- artifact

Image and labels have then been converted into the relative TensorFlow formats: images into the TensorFlow record, and labels into Comma Separated Values (CSV) listing: each row of the CSV contains the filename, the image dimensions, the label and the top-left and bottom-right corner of the object determined by the domain expert.

An excerpt from the above CSV file is shown in figure 2.

3.3 CNN for cell detection and classification

We have then trained a Faster R-CNN that uses two modules, a deep fully convolutional network that proposes regions, and another module is the Fast Region Convolutional Neural Network detector using the proposed regions [12]. Specifically we selected the Inception Resnet v2 model, using TensorFlow GPU [1]. The inference graph produced has been exported and tested using new sample, that is on the validation set.

4 Results

4.1 CNN Training

A double test has been performed, due to the fact that images were obtained using two different inverted optical microscopes with grayscale and RGB, with green background density, respectively.

train_labels.csv

```
filename,width,height,class,xmin,ymin,xmax,ymax
MG63_10x_08.jpg,1280,960,cancer_cluster,124,785,279,904
MG63_10x_08.jpg,1280,960,cancer_cluster,7,80,600,540
MG63_10x_08.jpg,1280,960,cancer_cluster,459,511,782,842
MG63_10x_08.jpg,1280,960,cancer_cluster,780,150,911,557
MG63_10x_08.jpg,1280,960,cancer,124,447,286,575
MG63_10x_08.jpg,1280,960,cancer,563,198,653,353
MG63_10x_08.jpg,1280,960,cancer,999,103,1091,279
MG63_10x_08.jpg,1280,960,cancer_cluster,929,264,1211,465
MG63_10x_08.jpg,1280,960,artifact,408,775,446,823
MG63_10x_08.jpg,1280,960,artifact,1250,847,1277,906
MG63_10x_08.jpg,1280,960,artifact,1111,61,1155,97
MG63_10x_06.jpg,1280,960,cancer_cluster,115,158,570,444
MG63_10x_06.jpg,1280,960,artifact,852,531,936,615
MG63_10x_06.jpg,1280,960,cancer_cluster,253,493,563,940
MG63_10x_06.jpg,1280,960,cancer_cluster,1003,387,1241,676
MG63_10x_06.jpg,1280,960,cancer_cluster,122,547,242,690
MG63_10x_10.jpg,1280,960,cancer_cluster,14,390,171,577
MG63_10x_10.jpg,1280,960,cancer_cluster,122,145,513,394
MG63_10x_10.jpg,1280,960,cancer_cluster,511,36,788,310
MG63_10x_10.jpg,1280,960,cancer_cluster,765,508,1148,866
MG63_10x_10.jpg,1280,960,cancer_cluster,258,604,690,954
MG63_10x_10.jpg,1280,960,cancer_cluster,363,398,682,644
MG63_10x_10.jpg,1280,960,artifact,194,64,282,139
MG63_10x_10.jpg,1280,960,cancer_cluster,745,150,1279,509
MG63_10x_10.jpg,1280,960,cancer_cluster,796,1,997,342
MG63_10x_10.jpg,1280,960,cancer_cluster,580,417,950,509
MG63_10x_10.jpg,1280,960,artifact,733,776,860,856
MSC_20x_01.jpg,1280,960,MSC,283,112,664,282
MSC_20x_01.jpg,1280,960,MSC,428,93,834,595
MSC_20x_01.jpg,1280,960,MSC,417,598,802,863
MSC_20x_01.jpg,1280,960,MSC_cluster,882,453,1271,960
MSC_20x_01.jpg,1280,960,artifact,538,178,588,238
MSC_20x_01.jpg,1280,960,artifact,234,297,411,435
MSC_20x_01.jpg,1280,960,artifact,226,716,383,850
MSC_20x_01.jpg,1280,960,artifact,34,178,220,286
MSC_20x_01.jpg,1280,960,artifact,809,23,1029,72
MSC_10x_06.jpg,1280,960,MSC,514,315,738,461
MSC_10x_06.jpg,1280,960,MSC,129,753,272,956
MSC_10x_06.jpg,1280,960,MSC,1096,679,1224,806
```

Fig. 2. Excerpt of CSV file

Then images produced with both microscopes have been converted into grayscale using [4] and a new training has been performed.

The training phase lasted five days for both the training sets using 300 regions proposals and a random horizontal flip has been applied to increase the number of samples and accuracy.

Both the inference graphs produced have been exported and tested for inference on new samples.

The following is an example of localization and recognition using the first graph on a RGB image.

The following is an example of the second graph localization and recognition on another gray-scale image.

The training has been performed on a personal computer equipped with a 4 cores 8 threads Intel(R) Core(TM) i7-4770 CPU @ 3.40 with 16 Giga Bytes DDR3 of RAM, an Nvidia Titan X powered with Pascal, and Ubuntu 16.04 as operative system.

4.2 CNN accuracy

Accuracy of the first trained graph on RGB images tested only on the RGB images is 0.97.

Accuracy have been also checked on all the validation set and the results are:

- 1 error
- 1 not determined

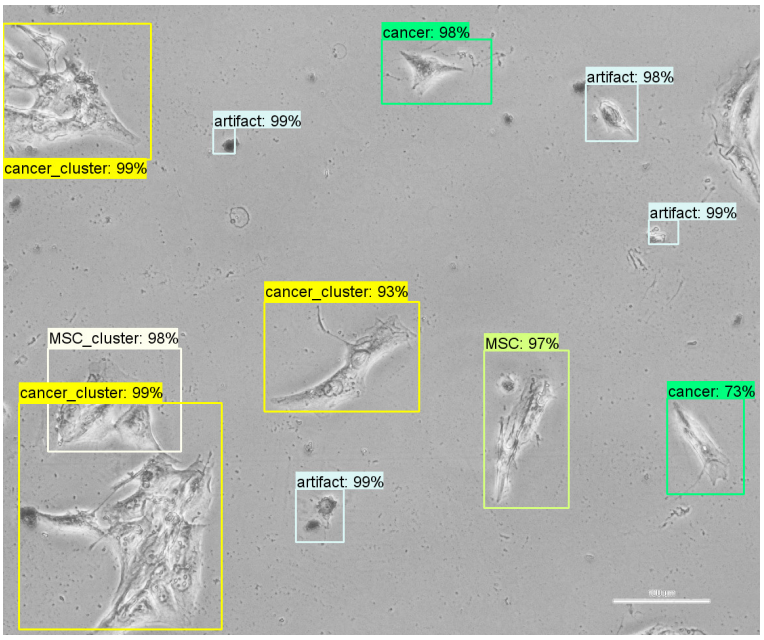

Fig. 3. An example of RGB image with localized and recognized objects under investigation. The ability of our method to discriminate between single or cell clusters is remarkable.

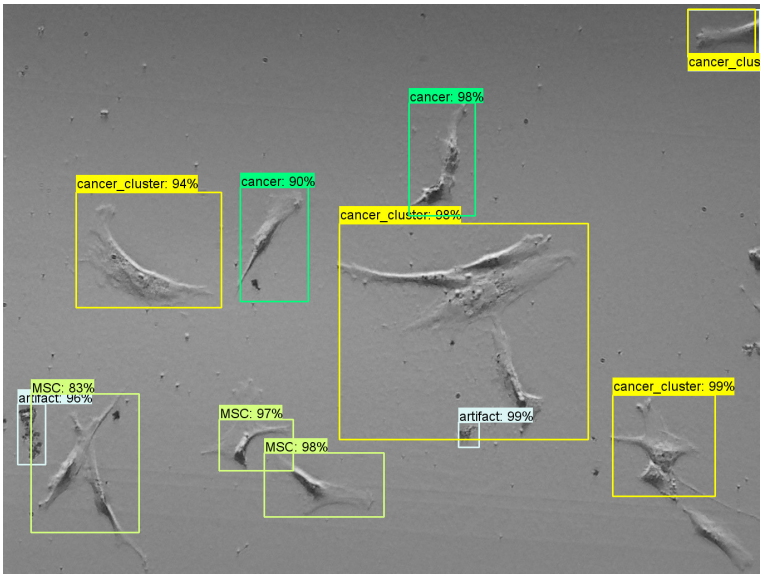

Fig. 4. An example of gray-scale image with localized and recognized objects under investigation. As in figure 3, the ability to discriminate between single and cell clusters is excellent.

With the second graph, obtained as the first one after 106000 cycles, the accuracy is again 0.97. By checking the inference on all the validation set we obtained the following results:

- 1 not determined
- 1 false positive

Figg. 3 and 4 show localized and recognized objects of the two training.

In figure 5 the trained graphs of the second test are shown: not only the Total Loss but also all the other region and box classification and localization graphs after 20,000 cycles tend to stabilize and then go close to zero.

On the basis of these results, the additional color layers seems not significant.

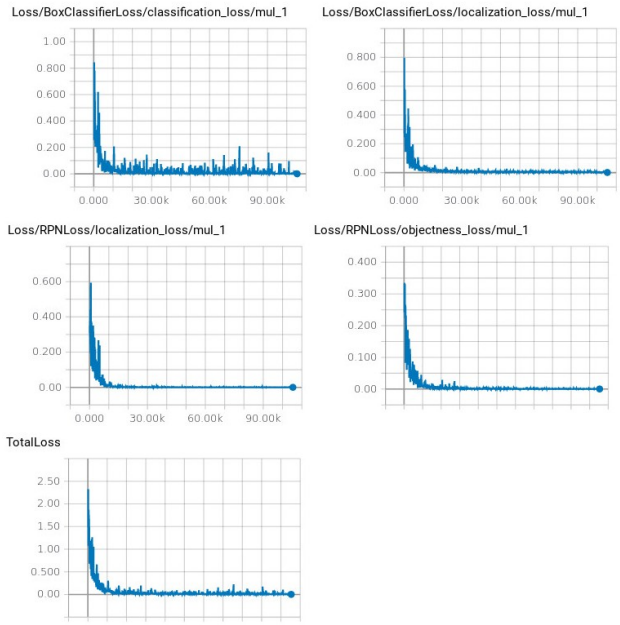

Fig. 5. Training graphs of the gray-scale test

Localization and recognition of new images require less than one second on a personal computer with a modern Intel I7 CPU.

5 Conclusions

Classification of single or small clusters of cancer cells is a crucial question for early diagnosis. In this paper, a Deep Learning approach to recognize single or small clusters of cancer cells have been presented. The Deep Learning method

adopted was based on Faster-RCNN technique. The ability of such algorithm to identify and classify approximately the 100% of the investigated cells potentially will allow us to extend the method to large population cells or tissues.

Acknowledgements

This work is being carried out in the framework of the BIO-ICT joint laboratory between the Institute of Biophysics and the Institute of Information Science and Technologies, both of the National Research Council of Italy, in Pisa.

We would like to thank Nvidia Corporation: this work would have required an invaluable time without a Titan X board powered by Pascal won by Signals & Images Laboratory of CNR-ISTI at the 2017 Nvidia GPU Grant.
We also wish to thank Luisa Trombi, Serena Danti, Delfo D'Alessandro, from University of Pisa, for useful support with biological samples.

References

1. Abadi, M., Barham, P., Chen, J., Chen, Z., Davis, A., Dean, J., Devin, M., Ghemawat, S., Irving, G., Isard, M., et al.: Tensorflow: A system for large-scale machine learning. In: OSDI, vol. 16, pp. 265–283 (2016)
2. Bychkov, D., Linder, N., Turkki, R., Nordling, S., Kovanen, P.E., Verrill, C., Walliander, M., Lundin, M., Caj, H., Lundin, J.: Deep learning based tissue analysis predicts outcome in cllorectal cancer. Scientifics Reports **8** (2018). DOI 10.1038/s41598-018-21758-3
3. Cireşan, D.C., Giusti, A., Gambardella, L.M., Schmidhuber, J.: Mitosis detection in breast cancer histology images with deep neural networks. In: International Conference on Medical Image Computing and Computer-assisted Intervention, pp. 411–418. Springer (2013)
4. Cristy, J.: Imagemagick website (2013). URL http://www.imagemagick.org/. Accessed 2018-06-08
5. Dürr, O., Sick, B.: Single-cell phenotype classification using deep convolutional neural networks. Journal of biomolecular screening **21**(9), 998–1003 (2016)
6. Huang, J., Rathod, V., Sun, C., Zhu, M., Korattikara, A., Fathi, A., Fischer, I., Wojna, Z., Song, Y., Guadarrama, S., Murphy, K.: Speed/accuracy trade-offs for modern convolutional object detectors. In: 2017 IEEE Conference on Computer Vision and Pattern Recognition, CVPR 2017, Honolulu, HI, USA, July 21-26, 2017, pp. 3296–3297 (2017). DOI 10.1109/CVPR.2017.351. URL https://doi.org/10.1109/CVPR.2017.351
7. Idikio, H.A.: Human cancer classification: A systems biology-based model integrating morphology, cancer stem cells, proteomics, and genomics. Journal of Cancer **2** (2011)
8. Li, Z., Soroushmehr, S.M.R., Hua, Y., Mao, M., Qiu, Y., Najarian, K.: Classifying osteosarcoma patients using machine learning approaches. In: 2017 39th Annual International Conference of the IEEE Engineering in Medicine and Biology Society (EMBC), pp. 82–85 (2017). DOI 10.1109/EMBC.2017.8036768
9. Mishra, R., Daescu, O., Leavey, P., Rakheja, D., Sengupta, A.: Convolutional neural network for histopathological analysis of osteosarcoma **25** (2017)

10. Mishra, R., Daescu, O., Leavey, P., Rakheja, D., Sengupta, A.: Histopathological diagnosis for viable and non-viable tumor prediction for osteosarcoma using convolutional neural network. In: Z. Cai, O. Daescu, M. Li (eds.) Bioinformatics Research and Applications, pp. 12–23. Springer International Publishing, Cham (2017)
11. Nahid, A.A., Mehrabi, M.A., Kong, Y.: Histopathological breast cancer image classification by deep neural network techniques guided by local clustering. BioMEd Research International **2018** (2018)
12. Ren, S., He, K., Girshick, R., Sun, J.: Faster r-cnn: Towards real-time object detection with region proposal networks. In: C. Cortes, N.D. Lawrence, D.D. Lee, M. Sugiyama, R. Garnett (eds.) Advances in Neural Information Processing Systems 28, pp. 91–99. Curran Associates, Inc. (2015). URL http://papers.nips.cc/paper/5638-faster-r-cnn-towards-real-time-object-detection-with-region-proposal-networks.pdf
13. Ren, S., He, K., Girshick, R., Sun, J.: Faster r-cnn: towards real-time object detection with region proposal networks. IEEE transactions on pattern analysis and machine intelligence **39**(6), 1137–1149 (2017)
14. Song, Q., Merajver, S.D., Li, J.Z.: Cancer classification in the genomic era: five contemporary problems. Human Genomics **9** (2015)
15. Trombi, L., Mattii, L., Pacini, S., D'alessandro, D., Battolla, B., Orciuolo, E., Buda, G., Fazzi, R., Galimberti, S., Petrini, M.: Human autologous plasma-derived clot as a biological scaffold for mesenchymal stem cells in treatment of orthopedic healing. Journal of Orthopaedic Research **26**(2), 176–183 (2008)
16. Tzutalin: Labelimg. git code. https://github.com/tzutalin/labelImg (2015). Last accessed 11 May 2018
17. Uijlings, J., van de Sande, K., Gevers, T., Smeulders, A.: Selective search for object recognition. International Journal of Computer Vision (2013). DOI 10.1007/s11263-013-0620-5. URL http://www.huppelen.nl/publications/selectiveSearchDraft.pdf
18. Xie, Y., Xing, F., Kong, X., Su, H., Yang, L.: Beyond classification: structured regression for robust cell detection using convolutional neural network. In: International Conference on Medical Image Computing and Computer-Assisted Intervention, pp. 358–365. Springer (2015)